

AD-A056 006

ARMY ENGINEER TOPOGRAPHIC LABS FORT BELVOIR VA

F/G 14/5

AN EVALUATION OF THE METHOD OF DETERMINING PARALLAX FROM MEASUR--ETC(U)

DEC 77 M A CROMBIE, R S RAND

UNCLASSIFIED

ETL-0145

NL

1 OF 1  
AD  
A056006

ETL





ADA056006

ETL-0145

LEVEL

12

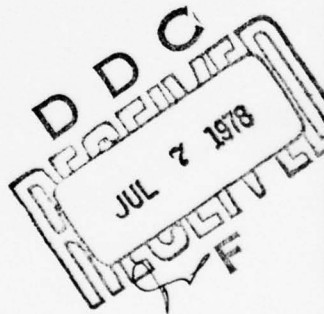


An evaluation of the method  
of determining parallax from  
measured phase differences

Michael A. Crombie      Robert S. Rand

DECEMBER 1977

AD No. \_\_\_\_\_  
DDC FILE COPY



78 07 06 005

U.S. ARMY CORPS OF ENGINEERS  
ENGINEER TOPOGRAPHIC LABORATORIES  
FORT BELVOIR, VIRGINIA 22060

E

T

L

Destroy this report when no longer needed.  
Do not return it to the originator.

---

The findings in this report are not to be construed as an official  
Department of the Army position unless so designated by other  
authorized documents.

---

The citation in this report of trade names of commercially available  
products does not constitute official endorsement or approval of the  
use of such products.

---



UNCLASSIFIED

SECURITY CLASSIFICATION OF THIS PAGE (When Data Entered)

REPORT DOCUMENTATION PAGE		READ INSTRUCTIONS BEFORE COMPLETING FORM
1. REPORT NUMBER 147 ETL-0145	2. GOVT ACCESSION NO.	3. RECIPIENT'S CATALOG NUMBER
4. TITLE (and Subtitle) 6 AN EVALUATION OF THE METHOD OF DETERMINING PARALLAX FROM MEASURED PHASE DIFFERENCES.	5. TYPE OF REPORT & PERIOD COVERED 9 Research Note	
7. AUTHOR(s) 10 Michael A. Crombie and Robert S. Rand.	6. PERFORMING ORG. REPORT NUMBER	
9. PERFORMING ORGANIZATION NAME AND ADDRESS Computer Sciences Laboratory U.S. Army Engineer Topographic Laboratories Fort Belvoir, VA 22060	8. CONTRACT OR GRANT NUMBER(s)	
11. CONTROLLING OFFICE NAME AND ADDRESS U.S. Army Engineer Topographic Laboratories Fort Belvoir, VA 22060	10. PROGRAM ELEMENT, PROJECT, TASK AREA & WORK UNIT NUMBERS 63701BR3202BB20	
14. MONITORING AGENCY NAME & ADDRESS (if different from Controlling Office)	12. REPORT DATE 11 December 1977	
	13. NUMBER OF PAGES 30 12/33	
	15. SECURITY CLASS. (of this report) Unclassified	
15a. DECLASSIFICATION/DOWNGRADING SCHEDULE		
16. DISTRIBUTION STATEMENT (of this Report)  Approved for public release; distribution unlimited.		
17. DISTRIBUTION STATEMENT (of the abstract entered in Block 20, if different from Report)		
18. SUPPLEMENTARY NOTES		
19. KEY WORDS (Continue on reverse side if necessary and identify by block number)  Autocorrelation      Fourier Transform Parallax Phase Shifts Epipolar Scans		
20. ABSTRACT (Continue on reverse side if necessary and identify by block number)  The practicality of determining parallax by means of detecting phase differences extracted from corresponding epipolar scans was evaluated using a digitized aerial image. The method was found to be not as accurate and not as efficient as conventional image matching techniques.		

## PREFACE

The work covered by this Research Note was conducted by the Computer Sciences Laboratory, (CSL), U.S. Army Engineer Topographic Laboratories, Fort Belvoir, Virginia. It is part of an effort being carried out in CSL on digital image analysis under project No. 63701BR3202BB20, Photogrammetric Exploitation. Studies were conducted by Michael A. Crombie and Robert S. Rand.

ACCESSION for	
NTIS	White Section <input checked="" type="checkbox"/>
DDC	Buff Section <input type="checkbox"/>
UNANNOUNCED	<input checked="" type="checkbox"/>
JUSTIFICATION	
BY	
DISTRIBUTION/AVAILABILITY CODES	
D.	SPECIAL
A	

78 07 06 005

## CONTENTS

Title	Page
<b>PREFACE</b>	1
<b>ILLUSTRATIONS</b>	3
<b>TABLES</b>	4
<b>INTRODUCTION</b>	5
<b>GEOMETRIC DESCRIPTION</b>	5
Epipolar Geometry	5
Fourier Representation	8
Phase Shift and Parallax	8
<b>NUMERICAL EXPERIMENT</b>	9
Weights	10
Window Size	11
<b>EVALUATION</b>	12
Fourier Model	12
Stereo	13
Numerical Results	13
<b>CONCLUSIONS</b>	21
<b>APPENDIX</b>	22

## ILLUSTRATIONS

Figure	Title	Page
1	Epipolar Geometry	6
2	Epipolar Scans	7

## TABLES

Table	Title	Page
1	Pull In Range	12
2	Image Scale Change At Middle of Model	13
3	Line Pairs Per Millimeter	14
4	$\sigma$ For L = 16	15
5	$\sigma$ For L = 32	15
6	$\sigma$ For L = 64	15
7	$\sigma$ For L = 128	16
8	$\sigma$ For L = 256	16
9	$\sigma/ s $ For L = 16	16
10	$\sigma/ s $ For L = 32	16
11	$\sigma/ s $ For L = 64	18
12	$\sigma/ s $ For L = 128	18
13	$\sigma/ s $ For L = 256	19
14	Average Values of $\sigma/ s $	19



## AN EVALUATION OF THE METHOD OF DETERMINING PARALLAX FROM MEASURED PHASE DIFFERENCES

### INTRODUCTION

The purpose of the report is to describe an evaluation of the practicality of determining parallax by means of detecting phase differences extracted from corresponding digital signals. The plan was to perform a preliminary evaluation by registering an image to itself using measured phase differences and if the test results proved promising, the plan was to enlarge the scope of the tests to include stereo images. Stereo tests were not performed because the initial results demonstrated that conventional autocorrelation methods were more accurate and more practical than measuring parallax by comparing phase differences.

The term autocorrelation in this report pertains to the process of establishing correspondence between identical image pairs. Conventional digital autocorrelation processes involve determining maximum or minimum points of discrete functions. The functions are generated by using any one of several measures of similarity, e.g. the linear correlation coefficient described in the Appendix. The term crosscorrelation pertains to the process of establishing correspondence between dissimilar images, e.g. stereo images. Conventional digital crosscorrelation processes are identical to conventional autocorrelation processes except that input data is extracted from corresponding scenes rather than from identical scenes.

### GEOMETRIC DESCRIPTION

In the proposed evaluation, corresponding lines of image data are extracted from stereo exposures, and specific points on the lines are brought into correspondence by signal matching in frequency space.

Epipolar Geometry. Consider two overlapping frame camera exposures. An epipolar line pair results from the intersection of the associated epipolar plane and the two focal planes. An epipolar plane is any member of the family of planes defined by the straight line connecting the two exposure positions. The corresponding epipolar section is the planar space curve defined by the epipolar plane and the surface of the earth. Then, except for points obscured by terrain heights, a one-to-one correspondence exists between the image points on epipolar line pairs and the associated object space point found on the epipolar section (See figure 1).

Suppose that  $P_1$  is selected on the first image and that the epipolar lines are constructed, then the corresponding image point  $P_2$  is somewhere on the second epipolar line. Thus, if the epipolar lines can be constructed, only a one-dimensional search need be conducted for  $P_2$ . Epipolar lines can be determined if the relative orientation of the two exposures is known.

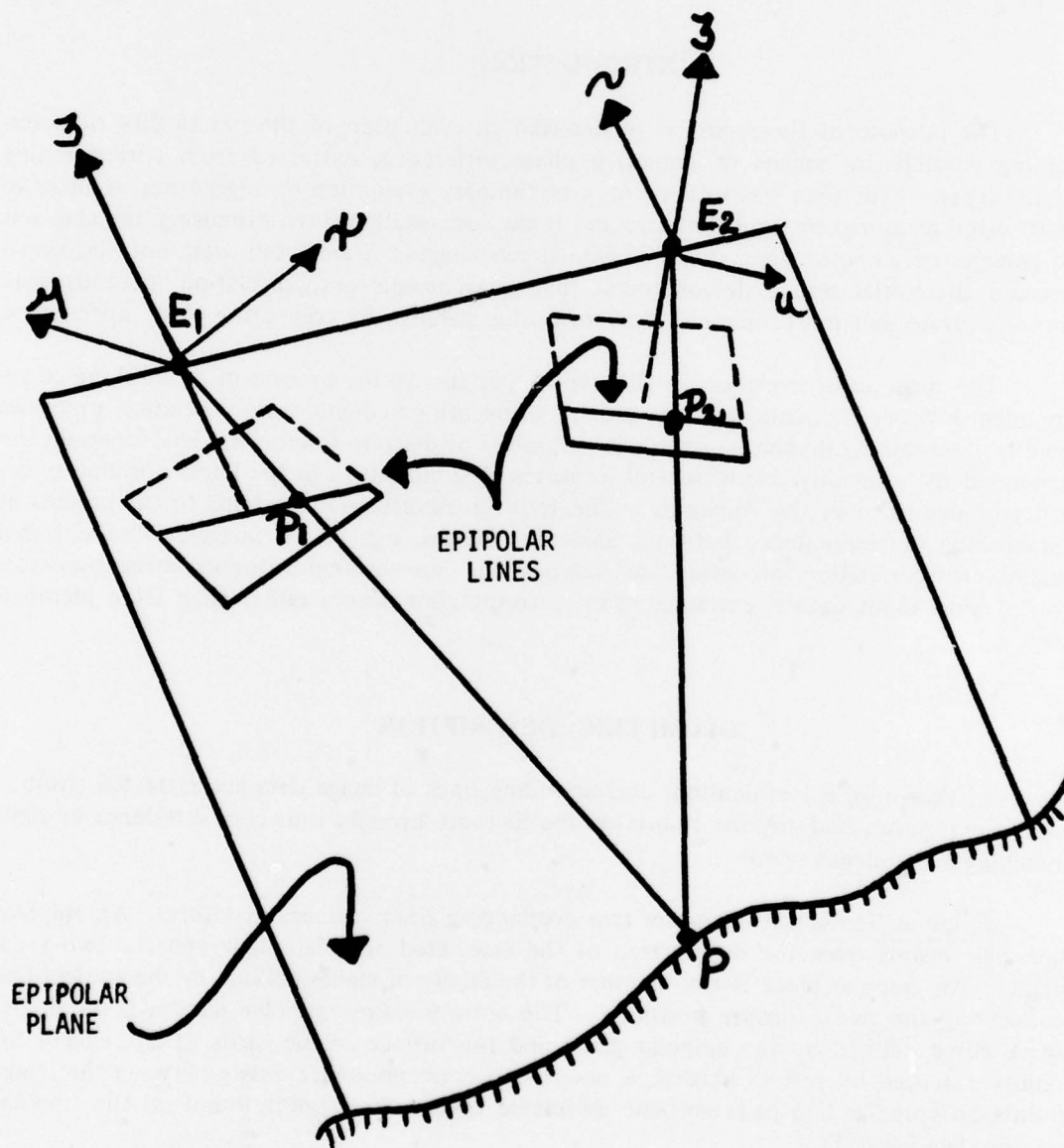
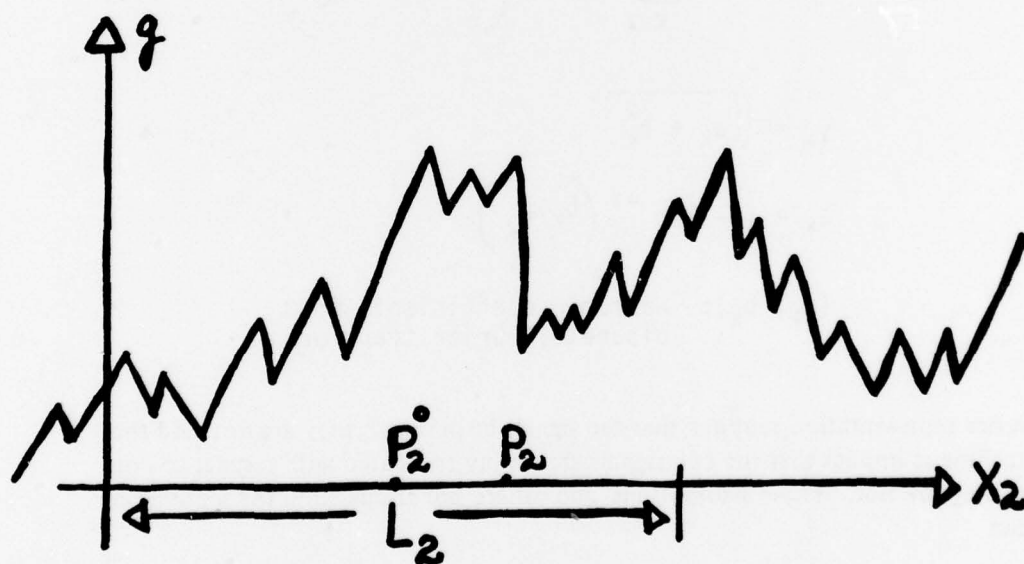
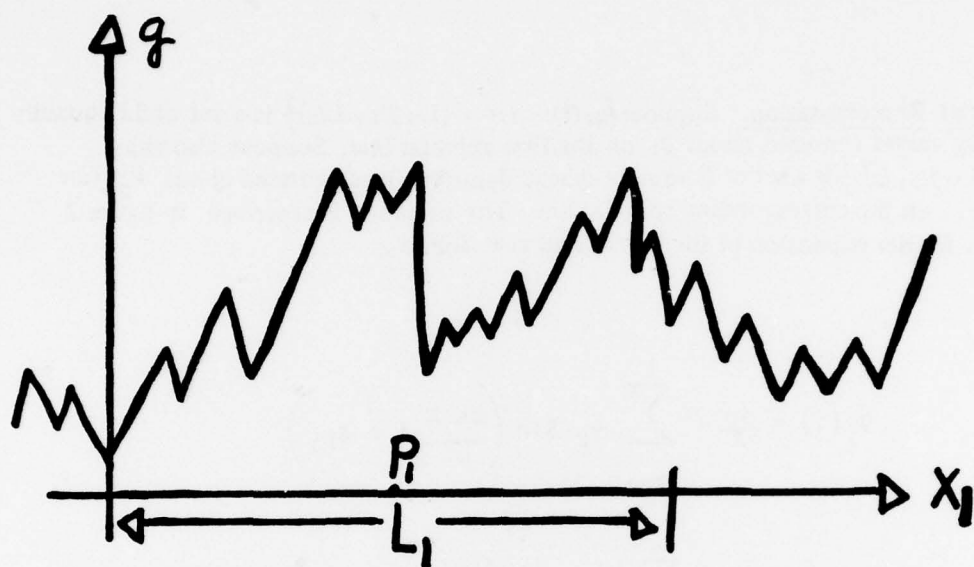


FIGURE 1. EPIPOLAR GEOMETRY.



$P_1$  : POINT DEFINED ON IMAGE #1

$P_2$  : CORRESPONDING POINT ON IMAGE #2

$P_2^0$  : ASSUMED MATCH POINT

$\Delta X = P_2 - P_2^0$  : X-PARALLAX

$L$  : LENGTH OF SCAN

FIGURE 2. EPIPOLAR SCANS.



Fourier Representation. Suppose  $\{g_1(i): i = -(L-1)/2, L/2\}$  is a set of  $L$  equally spaced density values centered about  $P_1$  on the first epipolar line. Suppose also that  $\{g_2(i): i = -(L-1)/2, L/2\}$  is a set of  $L$  equally spaced density values centered about  $P_2^0$  (an estimate of  $P_2$  on the corresponding epipolar line. The situation is described in figure 2 below. The fourier expansion of the two signals is as follows:

$$g_1(i) = \frac{a_0}{2} + \sum_{K=1}^L \gamma_K \sin\left(\frac{2K\pi}{L} i + \delta_{K1}\right)$$

$$g_2(i) = \frac{a_0}{2} + \sum_{K=1}^L \gamma_K \sin\left(\frac{2K\pi}{L} i + \delta_{K2}\right)$$

$$\gamma_K = \sqrt{a_K^2 + b_K^2}$$

$$\delta_K = \frac{\pi}{2} - \tan^{-1}\left(b_K/a_K\right)$$

$(a_K, b_K)$ : Harmonic coefficients from discrete Fourier transform

The Fourier representation requires that the signals be periodic, they are not; and the match technique implies that the two signals are simply translated with respect to one another, they are not. These assumptions, and others, are discussed in the section on evaluation.

Phase Shift and Parallax. From figure 1, the two curves can be brought into registration by translating the origin of  $g_2(i)$  by  $\Delta X = P_2 - P_2^0$  or by letting  $i = i' + \Delta X$ .

$$\begin{aligned} g_2(i) &= \frac{a_0}{2} + \sum_{K=1}^L \gamma_K \sin\left(\frac{2K\pi}{L} (i' + \Delta X) + \delta_{K2}\right) \\ &= \frac{a_0}{2} + \sum_{K=1}^L \gamma_K \sin\left(\frac{2K\pi}{L} i' + \left[\frac{2K\pi}{L} \Delta X + \delta_{K2}\right]\right) \end{aligned}$$

If  $g_1(i) = g_2(i)$  then

$$\delta K_1 = \frac{2K\pi}{L} \Delta X_K + \delta K_2$$

for each harmonic K.

$$\Delta X_K = \left( \frac{\delta K_1 - \delta K_2}{2K\pi} \right) L$$

The parallax value  $\Delta X$  can be estimated from each of the L harmonics. A weighted estimate of  $\Delta X$  will be calculated from Q of the harmonics.

$$\Delta X = \frac{\sum_Q W_Q \Delta X_Q}{\sum_Q W_Q} = 1$$

The weights will be defined in the next section.

## NUMERICAL EXPERIMENTS

The digitized image used for this experiment is stored in the DIAL<sup>1</sup> (Digital Image Analysis Laboratory) system, and it is described in a previous ETL report.<sup>2</sup> The digital image is a subimage taken from an exposure of rugged terrain. The essential features of the digitized model are

### Exposure Data

Camera Type: Vertical Frame  
Focal Length: 6 inches (15.2 cm)  
Scale : 1:48000

<sup>1</sup>Lawrence A. Gambino and Bryce L. Schrock, "An Experimental Digital Interactive Facility", Computer, Vol. 10, No. 8, August 1977, pp. 22-28.

<sup>2</sup>Michael Crombie, Stereo Analysis of A Specific Digital Model Sampled From Aerial Imagery, U.S. Army Engineer Topographic Laboratories, Fort Belvoir, Va., ETL-0072, September 1976 AD-A033 567.

### Digital Data

Image Dimension: 2048 x 2048  
 Grayshades : 256  
 Spot Diameter : 34.5  $\mu\text{m}$  (micrometers)  
 Spot Spacing : 24  $\mu\text{m}$

The experiment was one of autocorrelation; therefore, there was no need to extract epipolar line data. Approximately 25 lines of data were used in the tests. The lines were chosen to reflect a large range in signal power. Essentially, a line of  $(L + 2S)$  pixel values was extracted from the digital image on disc. The center of the line was designated as the test point  $P_1$ ; the image point  $P_1$  was characterized by a window of  $L$  pixels about it. The corresponding point  $P_2$  was defined to be at location  $(P_1 + s)$ , where  $s$  varied from zero to  $S$ . The image point  $P_2$  was also characterized by a window of  $L$  pixels about it. The match technique was applied to the two sets of pixels to determine how accurately the induced shift of  $\pm s$  could be recovered.

Weights. Two weighting functions were tested in this experiment. The first was derived from least squares, and the second was an empirical one that was simpler to compute. It can be shown that if the harmonic coefficients are computed by least squares, then the standard error of the parameter  $\delta_k$  is

$$\sigma_{\delta_k} = \frac{2\sigma_0}{\sqrt{N} \gamma_k}$$

$$\gamma_k = \sqrt{a_k^2 + b_k^2}$$

$\sigma_0$ : Standard error of the noise associated with the  $g(i)$ .

$N$  : Number of data points,  $L$  in this case.

If the noise is the same for both scans, then it can be also show that the standard error of the parallax is

$$\sigma_{\Delta X_K} \sim \frac{2 \sqrt{2} L \sigma_0}{\sqrt{N} \gamma_K \pi}$$

If the parallax value  $\Delta X$  is determined by least squares from  $Q$  of the  $\Delta X_K$  values and if the  $\Delta X_K$  are weighted according to  $\sigma \Delta X_K$  above, then the individual weights are

$$Wq(1) = \frac{1 / \sigma^2 \Delta X_q}{\sum_Q \frac{1}{\sigma^2 \Delta X_q}}$$

where  $q$  is the specific harmonic number. or

$$Wq(1) = \frac{q^2 \gamma_q^2}{\sum_Q q^2 \gamma_q^2}$$

The second weight function was defined to be

$$Wq(2) = \frac{\gamma_q^2}{\sum_Q \gamma_q^2}$$

Window Size. The window size  $L$  was allowed to vary, as was the input shift  $s$ .

$L = 16, 32, 64, 128, 256$  pixels

$s = 0, \pm 1, \pm 2, \dots, \pm 7$  pixels

Note that the window size was increased in length and the pixel spacing remained the same. A fast Fourier transform routine from the *DIAL* system was used to compute the required transform data.

## EVALUATION

If two sinusoids are out of phase by  $\frac{1}{4}$  period, then the cross-correlation is zero, and the pull-in range can be represented by the width of the correlation function. Table 1 represents PR, the pull-in range for the image used in the tests.

TABLE 1. PULL IN RANGE

<u>lp/mm</u>	<u>PR <math>\mu\text{m}</math></u>	<u>Pixels</u>
1	$\pm 250$	$\pm 10.0$
2	$\pm 125$	$\pm 5.0$
5	$\pm 50$	$\pm 2.0$
7	$\pm 35$	$\pm 1.5$
10	$\pm 25$	$\pm 1.0$
20	$\pm 13$	$\pm 0.5$

Generally, the lower frequencies have more signal power associated with them and, therefore, carry more weight in the shift calculations. Because of their lower power, the higher frequencies are more adversely affected by noise than are the lower frequencies. The fact the signal and its corresponding shifted signal are not periodic introduces a distortion into the calculations. If, in the stereo case, unshaped data are used, then an additional distortion will be introduced.

Fourier Model. The fact that image signals are not periodic caused most of the inconsistency in the method. The consistency of the computed shifts  $\Delta X_K$  turned out to be highly dependent upon the consistency of the signal power SP, as the window was displaced  $\pm s$  in the pixel direction. Signal power is defined here as the mean squared variation of the AC terms, or simply as the variance of the signal.

$$SP = \frac{\sum (g - \bar{g})^2}{L - 1}$$



If there was little or no change in SP as the induced shift  $s$  varied over its range, then the match results were accurate and precise. If SP changed by 10 percent or more, the computed  $\Delta X_K$  varied significantly in precision, and in many cases appeared to be erratic.

Stereo. Consider a ramp-like object imaged on two overlapping vertical frame images. If  $\alpha$  represents the tilt of the ramp with respect to the datum and B/H represents the imaging base-height ratio, then the entries in table 2 represent scale differences between the two images when the object is located in the middle of the model. For example, if  $\alpha = 20^\circ$  and B/H = 1, then the ramp image length on one exposure is 1.44 times the image length on the second exposure. It is assumed here that the ramp is aligned in the epipolar direction. More examples of scale distortion are given by Crombie and Gambino.<sup>3</sup>

TABLE 2. IMAGE SCALE CHANGE AT MIDDLE OF MODEL

B/H	$\alpha$						
	$0^\circ$	$5^\circ$	$10^\circ$	$15^\circ$	$20^\circ$	$25^\circ$	$30^\circ$
0.4	1.00	1.04	1.07	1.11	1.16	1.21	1.26
0.6	1.00	1.05	1.11	1.17	1.25	1.33	1.42
0.8	1.00	1.07	1.15	1.24	1.34	1.46	1.60
1.0	1.00	1.09	1.19	1.31	1.44	1.61	1.81

As shown in table 2, unless one image is stretched to accommodate the scale change, a large amount of signal difference for comparable scan lengths will occur, especially for large values of  $\alpha$  and B/H.

Numerical Results. The results given in table 3 pertain to  $Wq(1)$ , the first weighting method. This procedure turned out to be only slightly better than  $Wq(2)$ . The results are presented as a function of  $Q$  and  $L$ , where  $Q$  is the number of harmonics used in the estimate and  $L$  is the window length. It should be noted that it is not entirely correct to compare results over  $L$ . (See table 3).

<sup>3</sup>Michael A. Crombie and Lawrence A. Gambino, "Digital Stereo Photogrammetry", U.S. Army Engineer Topographic Laboratories, Fort Belvoir, Virginia, Presented at the Congress of the International Federation of Surveyors, Commission V, Stockholm, Sweden, June 1977.

TABLE 3. LINE PAIRS PER MILLIMETER

<u>L</u>	<u>H</u>			
	<u>1</u>	<u>3</u>	<u>5</u>	<u>7</u>
16	2.8	8.3	13.9	19.5
32	1.3	4.0	6.7	9.4
64	0.7	2.0	3.3	4.6
128	0.3	1.0	1.7	2.3
256	0.2	0.5	0.8	1.1

The entries in table 3 are line pairs per millimeter (lp/mm). They were calculated by converting the window lengths into millimeters and then computing the number of complete cycles per millimeter as a function of the harmonic number H. For example, the third harmonic pertains to 4 lp per mm when  $L = 32$  and to 1 lp per mm when  $L = 128$ . Thus, when  $Q = 7$  and  $L = 32$ , resolution information from 1.3 to 9.4 lp per mm is used to measure parallax; whereas, when  $Q = 7$  and  $L = 128$ , the resolution information ranges from 0.3 to 2.3 lp per mm.

Tables 4 through 8 represent sample standard errors of mismatch. The tabular parameters are defined as

S: True mismatch in pixels.

Q: Number of harmonics used in the weighted average. The first weight method (modified least squares) was used. For example, if  $Q = 5$ , then the shift was estimated from the first 5 harmonics.

L: Length of the window in pixels.

$\sigma$ : Estimated standard error with approximately 50 degrees of freedom. The standard error is expressed in pixels.

TABLE 4.  $\sigma$  For  $L = 16$ 

	Q				
<u>S</u>	<u>1</u>	<u>3</u>	<u>5</u>	<u>7</u>	
<u>+ 1</u>	0.76	0.49	0.47	0.58	

TABLE 5.  $\sigma$  For  $L = 32$ 

	Q				
<u>S</u>	<u>1</u>	<u>3</u>	<u>5</u>	<u>7</u>	
<u>+ 1</u>	0.59	0.38	0.32	0.35	
<u>+ 2</u>	1.22	0.80	0.73	0.81	

TABLE 6.  $\sigma$  For  $L = 64$ 

	Q				
<u>S</u>	<u>1</u>	<u>3</u>	<u>5</u>	<u>7</u>	
<u>+ 1</u>	0.50	0.40	0.36	0.33	
<u>+ 2</u>	0.91	0.76	0.71	0.65	
<u>+ 3</u>	1.33	1.08	1.07	0.99	
<u>+ 4</u>	1.84	1.40	1.50	1.66	



TABLE 7.  $\sigma$  For L = 128

Q				
<u>S</u>	<u>1</u>	<u>3</u>	<u>5</u>	<u>7</u>
<u>+ 1</u>	0.53	0.27	0.17	0.18
<u>+ 2</u>	1.04	0.57	0.37	0.39
<u>+ 3</u>	1.68	0.89	0.56	0.60
<u>+ 4</u>	2.03	1.19	0.74	0.78
<u>+ 5</u>	2.40	1.47	0.92	1.04
<u>+ 6</u>	2.43	1.73	1.08	1.20
<u>+ 7</u>	2.58	1.92	1.23	1.64

TABLE 8.  $\sigma$  For L = 256

Q				
<u>S</u>	<u>1</u>	<u>3</u>	<u>5</u>	<u>7</u>
<u>+ 1</u>	0.64	0.38	0.26	0.15
<u>+ 2</u>	1.41	0.73	0.52	0.30
<u>+ 3</u>	2.14	1.07	0.81	0.46
<u>+ 4</u>	2.56	1.25	1.13	0.62
<u>+ 5</u>	2.59	1.32	1.47	0.83
<u>+ 6</u>	2.61	1.59	1.54	1.00
<u>+ 7</u>	2.71	1.78	1.76	1.16

The quantity  $\sigma/|s|$  remains nearly constant as  $S$  varies and as  $Q$  is held constant. This observation is especially true for  $L \leq 128$  and is reasonably true for  $L = 256$ . Tables 9 through 13 demonstrate this observation. The value at the bottom of each column is the geometric mean of the tabular values.

TABLE 9.  $\sigma/|s|$  For  $L = 16$

		Q			
<u>S</u>	<u>1</u>	<u>3</u>	<u>5</u>	<u>7</u>	
<u>+ 1</u>	0.76	0.49	0.47	0.58	

TABLE 10.  $\sigma/|s|$  For  $L = 32$

		Q			
<u>S</u>	<u>1</u>	<u>3</u>	<u>5</u>	<u>7</u>	
<u>+ 1</u>	0.59	0.38	0.32	0.35	
<u>+ 2</u>	<u>0.61</u>	<u>0.40</u>	<u>0.32</u>	<u>0.41</u>	
	0.60	0.39	0.32	0.38	

TABLE 11.  $\sigma/|s|$  For  $L = 64$ 

<u>S</u>	Q			
	<u>1</u>	<u>3</u>	<u>5</u>	<u>7</u>
<u>+ 1</u>	0.50	0.40	0.36	0.33
<u>+ 2</u>	0.46	0.38	0.36	0.33
<u>+ 3</u>	0.44	0.36	0.36	0.33
<u>+ 4</u>	<u>0.46</u>	<u>0.35</u>	<u>0.38</u>	<u>0.42</u>
	0.47	0.37	0.37	0.35

TABLE 12.  $\sigma/|s|$  For  $L = 128$ 

<u>S</u>	Q			
	<u>1</u>	<u>3</u>	<u>5</u>	<u>7</u>
<u>+ 1</u>	0.53	0.27	0.17	0.18
<u>+ 2</u>	0.52	0.29	0.19	0.20
<u>+ 3</u>	0.56	0.30	0.19	0.20
<u>+ 4</u>	0.51	0.30	0.19	0.20
<u>+ 5</u>	0.48	0.29	0.18	0.21
<u>+ 6</u>	0.41	0.29	0.18	0.20
<u>+ 7</u>	<u>0.37</u>	<u>0.27</u>	<u>0.18</u>	<u>0.23</u>
	0.49	0.29	0.18	0.20

TABLE 13.  $\sigma/|s|$  For  $L = 256$ 

<u>S</u>	Q			
	<u>1</u>	<u>3</u>	<u>5</u>	<u>7</u>
<u>+ 1</u>	0.64	0.38	0.26	0.15
<u>+ 2</u>	0.71	0.37	0.26	0.15
<u>+ 3</u>	0.71	0.36	0.27	0.15
<u>+ 4</u>	0.64	0.31	0.28	0.16
<u>+ 5</u>	0.52	0.26	0.29	0.17
<u>+ 6</u>	0.44	0.27	0.26	0.17
<u>+ 7</u>	<u>0.39</u>	<u>0.26</u>	<u>0.25</u>	<u>0.17</u>
	0.59	0.32	0.27	0.16

Consider the average values of  $\sigma/|s|$  in table 14 and the 1p per mm relationship to specific harmonic values listed in table 3. A comparison of the two tables reveals that useful parallax information can be derived from image resolution content ranging from approximately 1 to about 10 lp per mm.

TABLE 14. AVERAGE VALUES OF  $\sigma/|s|$ 

<u>L</u>	Q			
	<u>1</u>	<u>3</u>	<u>5</u>	<u>7</u>
16	0.76	0.49	0.47	0.58
32	0.60	0.39	0.32	0.38
64	0.47	0.37	0.37	0.35
128	0.49	0.29	0.18	0.20
256	0.59	0.32	0.27	0.16

If subpixel precision is required and if the expected parallax  $S$  is up to 7 pixels or larger, then an averaging of parallax estimates at and around the point in question must be performed. This appears to be a valid approach owing to the observed variability of parallax estimates when a line is shifted in the pixel direction. This means that parallax estimates from adjacent lines should tend to be independent. The averaged parallax then will be the average shift over the area defined by the pixels used in the computation. Suppose  $M$  lines are averaged, the standard error of the parallax is required to be  $\xi * (\text{Pixel Spacing})$  where  $0 \leq \xi \leq 1$ , then  $M$  must satisfy the following relation.

$$M > \frac{E^2 * S^2}{\xi^2}$$

and suppose

$E$ : is the appropriate entry  
from Table 14

$S$ : is the expected shift

For example, suppose  $\xi = \frac{1}{4}$  pixel,  $L = 64$ ,  $S = \pm 4$  and  $Q = 7$ , then  $E = 0.35$  and  $M > 31$  lines. If in the same example  $S = \pm 7$ , then  $M > 86$  lines.

The results of this report pertain to autocorrelation. It has been shown that a large number of calculations need to be performed to calculate the induced shifts precisely. Even with identical images, an iterative approach must be performed to reduce the parallax error to zero. It should be noted that the computations can be performed efficiently in that algorithms can be developed where only those harmonics of interest need be computed. It should also be noted that if the same procedure were to be applied to stereo data, then the following error sources will increase the output error:

1. Comparing phase angles from different epipolar lines..
2. Comparing phase angles when one line is stretched with respect to the other.

The first error source derives from erroneous interior and exterior orientation data. The second error source occurs whenever the corresponding lines are not shaped accurately. When the parallax is significant, the second error source has the most effect on the output error.



The evaluation described in this report must be performed iteratively, possibly with diminishing window lengths  $L$ , to achieve zero error even in autocorrelation. If accurate and precise parallax estimates for stereo are to be computed in relatively steep terrain, then pixel shaping must be performed, with enough care taken in the scan procedure to ensure that corresponding epipolar lines are measured. If enough care is taken to produce corresponding epipolar lines and if the lines are shaped to reflect expected parallax, then conventional correlation methods are superior to frequency space matching. These are two reasons for this. First, correct shifts can be computed from a single correlation function in autocorrelation. Second, the algorithm (for stereo matching and for autocorrelation) can be organized so that every point on corresponding epipolar lines can be matched concurrently with great efficiency. The appendix contains the computer operations associated with this correlation procedure. A conventional correlation procedure using methods very similar to those in the appendix has been applied to the AS-11 B-X device that was developed by Bendix Corporation for the Defense Mapping Agency.<sup>4</sup> The great economy in computer operations is derived from the existence of significant quantities of identical calculations as the correlation process ranges over neighboring points. There is not a similar economy in the method described in this report. The utility of matching all possible points along the corresponding epipolar pair is realized when, as in practice, part of the line cannot be matched because of poor image detail or because of obscurations. The abundance of matched points can be used to interpolate for missing points and to provide a generally smoother set of output points.

## CONCLUSIONS

1. Most of the useful parallax information can be derived from image resolution content ranging from 1 to 10 lp per mm for the aerial image used in this report.
2. Measuring parallax by comparing phase differences between corresponding epipolar lines is greatly dependent upon stability in signal power as the matching line is shifted in the pixel direction.
3. If signal power changed by 10 percent or more, the computed parallax estimate varied significantly in precision and in many cases appeared to be erratic.
4. Measuring parallax by comparing phase differences is not as precise as conventional correlation methods in autocorrelation. It is expected to be even less precise in the stereo mode.
5. Measuring parallax by comparing phase differences does not offer computational advantages over conventional correlation methods.

---

<sup>4</sup>F. Scarano and G. Brumm "A Digital Elevation Data Collection System", Photogrammetric Engineer and Remote Sensing, Vol XLII, No. 4, April 1976.

## APPENDIX. Number of Computer Operations Needed For Vector Correlation

Given two N-dimensional corresponding epipolar lines of gray shades X and Y, suppose M adjacent points of Y are to be matched to M corresponding points of X. Assume too that X has been shaped approximately so that the M estimated match points of X are also adjacent points or nearly so. The correspondence will be refined by correlation methods where for each of the M matches, P correlation values will be calculated using a window of length W. If P and W are odd and if all possible points are matched, then  $M = N + 2 - W - P$ .

Essentially, M discrete correlation functions of dimension P will be developed where the central value of each pertains to the approximate match-point location. A shift S for each of the M approximations will be estimated by determining the location of the peak correlation value. The window length W must be large enough to produce precise correlation values, and the number of correlation values P must be large enough so that the extent of the correlation function covers the actual match location. If the largest possible shift in absolute value is SMAX, then  $(P-1)/2 > \text{SMAX}$ . The purpose of this appendix is to calculate the number of computer operations necessary to calculate the M correlation functions.

The measure of similarity used is the following linear correlation coefficient:

$$r_{ij} = \frac{\sum_{k=1}^W (X_{ijk} - \bar{X}_{ij}) (Y_{ijk} - \bar{Y}_{ij})}{\sqrt{\sum_{k=1}^W (X_{ijk} - \bar{X}_{ij})^2} \sqrt{\sum_{k=1}^W (Y_{ijk} - \bar{Y}_{ij})^2}}$$

Where

$$i = 1, M$$

$$j = 1, P$$

Any one of the required  $M * P$  correlation values can be computed from the following five basic quantities:

$$\sum_{k=1}^W x_{ijk}, \quad \sum_{k=1}^W x_{ijk}^2, \quad \sum_{k=1}^W y_{ijk}, \quad \sum_{k=1}^W y_{ijk}^2$$

and  $\sum_{k=1}^W x_{ijk} * y_{ijk}$

A straightforward count of the necessary number of computer operations is given first. No regard for computational overlap is taken into account. However, the next calculation pertains to the situation where all possible computational overlap is considered.

Straightforward Count. The subscripts on X and Y are dropped for convenience. The following counts of the number of add and multiply operations pertain to the five basic quantities given above.

$$\left. \begin{array}{l} \sum X : W \text{ adds} \\ \sum X^2 : W \text{ adds} \\ \quad \quad W \text{ multiplies} \end{array} \right\} * M * P$$

$$\left. \begin{array}{l} \sum Y : W \text{ adds} \\ \sum Y^2 : W \text{ adds} \\ \quad \quad W \text{ multiplies} \end{array} \right\} * M$$

$$\left. \begin{array}{l} \sum XY : W \text{ adds} \\ \quad \quad W \text{ multiplies} \end{array} \right\} * M * P$$



The total number of adds and multiplies for the five components is

$$T_A' = M * W * (3 * P + 2)$$

$$T_M' = M * W * (2 * P + 1)$$

The five components are combined in the following way to produce the correlation value r:

$$r = \frac{W \sum XY - \sum X \sum Y}{\sqrt{W \sum X^2 - (\sum X)^2} \sqrt{W \sum Y^2 - (\sum Y)^2}}$$

Each of the  $M * P$  numerators require one add and two multiplications for a total of

$M * P$  adds and

$2 * M * P$  multiplies.

Each of the  $M$  radicals involving  $Y$  require one add, two multiplies, and one square root for a total of

$M$  adds,

$2 * M$  multiplies and

$M$  square roots.

Each of the  $M * P$  radicals involving  $X$  require one add, two multiplies, and one square root for a total of

$M * P$  adds,

$2 * M * P$  multiplies and

$M * P$  square roots.

The total number of adds and multiplies for the five components is

$$T_A' = M * W * (3 * P + 2)$$

$$T_M' = M * W * (2 * P + 1)$$

The five components are combined in the following way to produce the correlation value r:

$$r = \frac{W \sum XY - \sum X \sum Y}{\sqrt{W \sum X^2 - (\sum X)^2} \sqrt{W \sum Y^2 - (\sum Y)^2}}$$

Each of the  $M * P$  numerators require one add and two multiplications for a total of

$M * P$  adds and

$2 * M * P$  multiplies.

Each of the  $M$  radicals involving  $Y$  require one add, two multiplies, and one square root for a total of

$M$  adds,

$2 * M$  multiplies and

$M$  square roots.

Each of the  $M * P$  radicals involving  $X$  require one add, two multiplies, and one square root for a total of

$M * P$  adds,

$2 * M * P$  multiplies and

$M * P$  square roots.

Each of the  $M * P$  denominators require one multiplication involving the two radicals, and finally each of the  $M * P$  correlation values require one division.

The total number of operations involved in combining the five components is

$$\begin{aligned} T_A'' &= M * (2 * P + 1) && \text{adds} \\ T_M'' &= M * (5 * P + 1) && \text{multiplies} \\ T_D'' &= M * P && \text{divides} \\ T_R'' &= M * (P + 1) && \text{square roots.} \end{aligned}$$

The number of operations used to calculate the five components are combined with these results to produce the total number of computer operations needed to develop the  $M$  correlation functions.

$$\begin{aligned} T_A &= M * [2 * P + 1 + W * (3 * P + 2)] && \text{adds} \\ T_M &= M * [5 * P + 1 + W * (2 * P + 1)] && \text{multiplies} \end{aligned}$$

$$\begin{aligned} T_D &= M * P && \text{divides} \\ T_R &= M * (P + 1) && \text{square roots.} \end{aligned}$$

Computational Overlap Considered. Most of the computational overlap occurs in the calculation of the five primary components given above. The computational overlap can be deduced by examining a simple example. Suppose,  $N = 9$ ,  $W = 3$ , and  $P = 5$ ; then  $M = 3$  and points 4, 5, and 6 of  $Y$  will be matched to corresponding points of  $X$ .

$$\begin{aligned} Y: & Y_1, Y_2, \dots, Y_9 \\ X: & X_1, X_2, \dots, X_9 \end{aligned}$$

The quantities needed to compute the five primary components for the three correlation functions are given next.

$$\underline{R(Y_4, X_4)}$$

$$\Sigma Y : (Y_3 + Y_4 + Y_5)$$

$$\Sigma Y^2 : (Y_3^2 + Y_4^2 + Y_5^2)$$

$$\Sigma X : (X_1 + X_2 + X_3), (X_2 + X_3 + X_4), (X_3 + X_4 + X_5), (X_4 + X_5 + X_6), \\ (X_5 + X_6 + X_7).$$

$$\Sigma X^2 : (X_1^2 + X_2^2 + X_3^2), (X_2^2 + X_3^2 + X_4^2), (X_3^2 + X_4^2 + X_5^2), (X_4^2 + X_5^2 + X_6^2), \\ (X_5^2 + X_6^2 + X_7^2).$$

$$\Sigma XY : (X_1 Y_3 + X_2 Y_4 + X_3 Y_5), (X_2 Y_3 + X_3 Y_4 + X_4 Y_5), (X_3 Y_3 + X_4 Y_4 + X_5 Y_5), \\ (X_4 Y_3 + X_5 Y_4 + X_6 Y_5), (X_5 Y_3 + X_6 Y_4 + X_7 Y_5).$$

$$\underline{R(Y_5, X_5)}$$

$$\Sigma Y : (Y_4 + Y_5 + Y_6)$$

$$\Sigma Y^2 : (Y_4^2 + Y_5^2 + Y_6^2)$$

$$\Sigma X : (X_2 + X_3 + X_4), (X_3 + X_4 + X_5), (X_4 + X_5 + X_6), (X_5 + X_6 + X_7), \\ (X_6 + X_7 + X_8).$$

$$\Sigma X^2 : (X_2^2 + X_3^2 + X_4^2), (X_3^2 + X_4^2 + X_5^2), (X_4^2 + X_5^2 + X_6^2), (X_5^2 + X_6^2 + X_7^2), \\ (X_6^2 + X_7^2 + X_8^2).$$

$$\Sigma XY : (X_2 Y_4 + X_3 Y_5 + X_4 Y_6), (X_3 Y_4 + X_4 Y_5 + X_5 Y_6), (X_4 Y_4 + X_5 Y_5 + X_6 Y_6), \\ (X_5 Y_4 + X_6 Y_5 + X_7 Y_6), (X_6 Y_4 + X_7 Y_5 + X_8 Y_6)$$

R (Y<sub>6</sub>, X<sub>6</sub>)

$$\Sigma Y : (Y_5 + Y_6 + Y_7)$$

$$\Sigma Y^2 : (Y_5^2 + Y_6^2 + Y_7^2)$$

$$\Sigma X : (X_3 + X_4 + X_5), (X_4 + X_5 + X_6), (X_5 + X_6 + X_7), (X_6 + X_7 + X_8) \\ (X_7 + X_8 + X_9)$$

$$\Sigma Y^2 : (X_3^2 + X_4^2 + X_5^2), (X_4^2 + X_5^2 + X_6^2), (X_5^2 + X_6^2 + X_7^2), (X_6^2 + X_7^2 + X_8^2) \\ (X_7^2 + X_8^2 + X_9^2)$$

$$\Sigma XY : (X_3 Y_5 + X_4 Y_6 + X_5 Y_7), (X_4 Y_5 + X_5 Y_6 + X_6 Y_7), (X_5 Y_5 + X_6 Y_6 + X_7 Y_7) \\ (X_6 Y_5 + X_7 Y_6 + X_8 Y_7), (X_7 Y_5 + X_8 Y_6 + X_9 Y_7)$$

The  $\Sigma Y$  value for the first correlation function can be developed by  $W$  adds, and the remaining  $\Sigma Y$  values for the  $(M-1)$  other correlation functions can be developed by two adds apiece for a total of  $W + 2 * (M-1)$  adds. The  $\Sigma Y$  value for  $R(Y_5, X_5)$  is computed by subtracting  $Y_3$  from and adding  $Y_6$  to the  $\Sigma Y$  value for  $R(Y_4, X_4)$ . The  $\Sigma Y$  value for  $R(Y_6, X_6)$  is computed by subtracting  $Y_4$  from and adding  $Y_7$  to the  $\Sigma Y$  value for  $R(Y_5, X_5)$ . The  $\Sigma Y^2$  values are developed in the same manner; the results for the  $\Sigma Y$  and  $\Sigma Y^2$  components are

$$\Sigma Y : W + 2 * (M-1) \text{ adds}$$

$$\Sigma Y^2 : W + 2 * (M-1) \text{ adds}$$

$$W + 2 * (M-1) \text{ multiplies}$$

The  $\Sigma X$  values can be computed even more efficiently than the  $\Sigma Y$  values. Consider the  $P = \text{five}$   $\Sigma X$  values for  $R(Y_4, X_4)$ . The first can be developed with  $W$  adds, and the remaining  $(P-1)$  values can be developed with two adds apiece for a total of  $W + 2 * (P-1)$  adds. Note that  $(P-1)$  of the  $\Sigma X$  values for  $R(Y_5, X_5)$  are identical to those of  $R(Y_4, X_4)$ , and the remaining  $\Sigma X$  value can be developed by two adds. The total number of adds for  $\Sigma X$  is  $W + 2 * (P-1) + 2 * (M-1)$ . The  $\Sigma X^2$  values are developed in the same way; the results for the  $\Sigma X$  and  $\Sigma Y^2$  values are



$$\sum X : W + 2 * (P-1) + 2 * (M-1) \text{ adds}$$

$$\begin{aligned} \sum X^2 : W + 2 * (P-1) + 2 * (M-1) \text{ adds} \\ W + 2 * (P-1) + 2 * (M-1) \text{ multiplies} \end{aligned}$$

There is no computational overlap for the  $\sum XY$  components within a specific correlation function, but there is computational overlap between correlation functions. The first correlation function will require  $W * P$  adds and  $W * P$  multiplies to compute the  $P \sum XY$  values. Each of the succeeding  $(M-1)$  correlation functions will require  $2 * P$  adds and  $P$  multiplications for a total of

$$\begin{aligned} \sum XY : W * P + 2 * P * (M-1) \text{ adds} \\ W * P + P * (M-1) \text{ multiplies} \end{aligned}$$

The total number of required adds and multiplies for the five components are

$$\begin{aligned} TA &= W * (P+4) + 2 * (M-1) * (P+4) + 4 * (P-1) \\ TM &= W * (P+2) + (M-1) * (P+4) + 2 * (P-1) \end{aligned}$$

Except for the radical involving  $X$ , the number of individual calculations (where the five components are combined to produce correlation values) is identical to the number of operations for the radical involving  $X$  is

$$\begin{aligned} M + P - 1 & \text{ adds} \\ 2 * M + 2 * (P-1) & \text{ multiplies and} \\ M + P - 1 & \text{ square roots.} \end{aligned}$$

The total number of computer operations involved in combining the five components is

$$\begin{aligned}
 T_A'' &= M * (P+2) + (P-1) \\
 T_M'' &= M * (3 * P + 4) + 2 * (P-1) \\
 T_D'' &= M * P \\
 T_R'' &= 2 * M + (P-1)
 \end{aligned}$$

The numbers of operations used to calculate the five components are combined with the results above to produce the total number of computer operations needed to develop the M correlation functions.

$$\begin{aligned}
 T_A &= [W + 3 * (M+1)] * P + (4 * W + 10 * M - 13) \\
 T_M &= [W + 4 * M + 3] * P + 2 * [W + 8 * (M - 1)] \\
 T_D &= M * P \\
 T_R &= 2 * M + (P - 1)
 \end{aligned}$$

The values  $R_A$ ,  $R_M$ ,  $R_D$ , and  $R_R$  are the multiplicative increases in compute operations when computational overlap is ignored. The value  $R_A$  (increase in number of adds) is computed by calculating the ratio of the two  $T_A$  values; the other ratios are calculated in the same manner.

$$R_A \sim \frac{(3 * P + 2) * W}{(3 * P + 10) + \frac{W}{N} * (P + 4)}$$

$$R_M \sim \frac{(2 * P + 1) * W}{(4 * P + 16) + \frac{W}{N} * (P + 2)}$$

$$R_D = 1$$

$$R_R \sim P/2$$

If, for example, N is very large compared to the window size W and if P is also large, then  $R_A \sim W$ ,  $R_M \sim W/2$  and  $R \sim P/2$ .